Neural Computing and Applications (2020) 32:15171–15189
https://doi.org/10.1007/s00521-020-04868-w

ORIGINAL ARTICLE

Fault classification in three-phase motors based on vibration signal analysis and artificial neural networks

Ronny Francis Ribeiro Junior[1,3] · Fabrício Alves de Almeida[2] · Guilherme Ferreira Gomes[1]

Received: 20 December 2019 / Accepted: 14 March 2020 / Published online: 27 March 2020

Abstract
Competition in the industrial environment is increasingly intense, so it is of utmost importance that organizations keep their assets in operation as much as possible (in order to produce more). In this context, there is a need for predictive maintenance, a technique that detects the health of assets in real time, allowing failures to be diagnosed before they can interrupt the operation of the assets, avoiding high financial losses. This study uses a sixteen-motor experimental setup with four different known operating conditions. The vibration signal of these motors, through signal analysis, both in time and frequency domains, is performed to evaluate the types and severities of the defects. An artificial neural network (ANN) is used to classify these defects. Considering the vibration analysis, mechanical faults can be identified quickly and conveniently. For the development of the ANN, it was necessary to perform a preprocessing of the vibration signal (response in time) due to the data size, which overwhelms the network. Thus, statistical data were used to extract key information from the vibration signal. Finally, the neural network created based on this study's methodology presents extremely reliable results, allowing a quick and robust diagnosis of the motor operating condition.

Keywords Predictive maintenance · Vibration analysis · FFT · Artificial neural networks · Damage classification

1 Introduction

Induction motors present high performance and reliability, playing a critical role in many industrial sectors. However, despite their reliability, they are subject to failure [26]. Being able to classify or predict failures (or operating condition) is a task of great importance and crucial for engineers, especially in the field of maintenance. One of the possible solutions is through the use of artificial neural networks (ANN) based on data from certain engines. An effective ANN is able to efficiently predict the assessed response saving time and maintenance costs.

Thus, the general industry's demand for predictive maintenance products and services is increasing. Predictive maintenance is one that indicates the actual operating conditions of equipment based on elements that report wear or degradation process. Therefore, long-term maintenance costs can be reduced with adequate predictive maintenance techniques [18].

In this context, the vibration analysis method is a mature and applicable alternative for predictive motor maintenance. There are two important steps to implement the fault diagnosis process: The first is signal processing and the second is signal classification based on the characteristics obtained in the previous step. The diagnosis is usually much more difficult than the detection because different failures may exhibit similar symptoms and multiple failures may occur at the same time [22].

Currently, artificial neural networks (ANN) techniques are attracting attention in studies given their ability to perform difficult tasks [5, 8, 12, 13], such as vibration signal diagnosis, quickly and efficiently [14, 23, 25, 26]. Therefore, a neural network can contribute to the speedy diagnosis of a failure by increasing the efficiency of predictive maintenance. Nevertheless, to the best of the authors' knowledge, very few efforts have been devoted to

✉ Guilherme Ferreira Gomes
guilhermefergom@unifei.edu.br

[1] Mechanical Engineering Institute, Federal University of Itajubá – UNIFEI, Itajubá, Brazil

[2] Institute of Industrial Engineering and Management, Federal University of Itajubá – NIFEI, Itajubá, Brazil

[3] PS Solutions, Itajubá, Brazil

the development of ANN-based vibration data of three-phase motors considering different experimental fault conditions.

The main objective of this monograph is to analyze the vibratory behavior of motors subject to different types of defects and classify them. The specific objectives of this study are: (i) Defect analysis using techniques such as FFT (*fast Fourier transform)*, evaluating the amplitude and operating frequency variations in the studied motor; (ii) create an artificial neural network capable of classifying defects in three-phase induction motors; and (iii) encourage the use of neural networks to assist vibration analysis, showing the importance of marrying both techniques.

In this paper, a dynamic experimental study of three-phase motors with different operating conditions is made. The results show a very good fault classification of these motors using ANN based on vibration signal data. Although many studies have been reported on the vibration analysis of rotating machines, very few have been focused on the fault classification using different defects types as presented in this manuscript. The work presented here assesses the potential of ANN for a fast fault classification in industry.

More specifically, the major contributions of this article are summarized as follows: (i) experimental tests evaluating four different operating conditions in 16 three-phase motors in terms of their vibratory responses; (ii) extraction of different statistical data from the vibration signal and evaluation through analysis of variance (ANOVA); and (iii) development of an ANN in order to classify the operating condition and defect.

This manuscript is organized as follows: In Sect. 2, a general bibliographic review is presented, addressing an overview of maintenance of the electrical motors in Brazil. Section 3 shows the background of ANN. In Sect. 4, the methodological procedure is presented. Section 5 presents the main results and discussion about the fault classification based on vibration data. Finally, Sect. 6 draws the conclusions.

2 Theoretical background

2.1 An overview of maintenance in electrical motors in Brazilian industries

According to Moubray [21] and Fogliatto and Ribeiro [10], the term maintenance is understood as the action of repairing or performing services on equipment and systems. Such actions have the sole purpose of ensuring that the equipment continues to perform its assigned activities. Brown [7] defines predictive maintenance as an approach that compares the tendency of measurements of the analyzed physical parameters (vibration, noise, temperature) with the limits established for these parameters, in order to detect, analyze and correct problems before they lead to failure of equipment.

From the 1930s, there was the beginning of concern with the maintenance of equipment. At that time, maintenance was limited only to repairs made after the breakdown of some equipment, which in most cases were simple and oversized [17, 21].

After the first and second war, there was an increase in mechanization and complexity of industrial facilities. With the large-scale production, there was even more the need to have greater availability and reliability of equipment. In this context, the replacement of parts and equipment begins before a possible breakdown, based on their expected lifetime [10, 17, 21].

In the mid-1970s, the process of change in organizations accelerated a change characterized by increased economic competitiveness. In this scenario, the concern with reliability and availability of equipment increased. Thus, a need arose for maintenance where possible failures could be identified before causing production stoppages and thus arose the maintenance model that seeks ways to foresee a possible break or stop and make the appropriate planning of relevant actions [2, 21, 24].

Currently, the concept of maintenance is even broader as it aims to reduce equipment failure and increase its availability by reducing the likelihood of failure. Also, the processes in companies are more mature in concepts like lean manufacturing, which makes machine reliability and availability more critical [2, 24].

As discussed, maintenance techniques have evolved according to the needs of industries. Thus, it is up to each company's maintenance staff to select the most cost-effective type of maintenance for each equipment within the organization. According to a study by the Brazilian Association of Maintenance and Asset Management [2], the sum of the corrective and preventive maintenance is 79% of all maintenances performed, which is a relatively high percentage that demonstrates the technological backwardness of the Brazilian industry in relation to the maintenance of its assets. Table 1 and Fig. 1 elucidate better Brazilian maintenance setting.

2.2 Maintenance on induction motors

Representing about 90% of all motors used in the world, three-phase induction motors are widely used due to their robustness, acceptable performance and low cost. Also, with the advent of speed and torque control systems applied to this type of motor, its use in critical processes or great importance in the industry is common.

An induction motor consists basically of two parts: the stator and the rotor. The stator is the static part and the

Table 1 Types of maintenance in each sector of Brazil's industry Adapted from [2]

Sector	Corrective (%)	Preventive (%)	Predictive (%)	Others (%)
Sugar and alcohol, food and beverage	42	40	18	0
Aeronautical and automotive	42	48	4	5
Consumer electronics—electric energy	28	44	12	16
Chemical and sanitation	25	50	20	5
Mining and steel	60	23	13	5
Petrochemical oil	47	39	14	0
Pulp and paper and plastic	24	31	31	14
Building and services (EQ and MO)	45	44	5	6
Machinery and equipment—metallurgical	25	48	7	20
Overall average	38	41	14	8

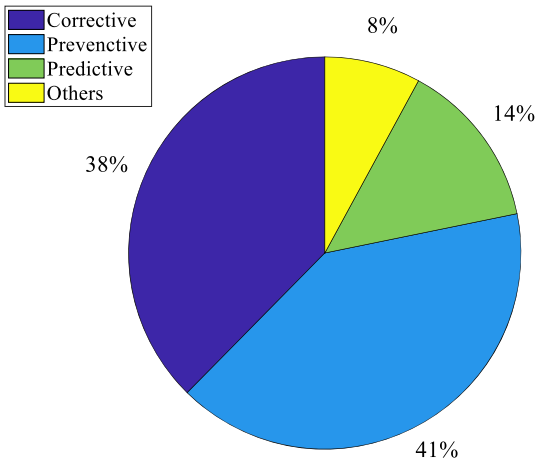

Fig. 1 General average of Brazilian maintenance. Adapted from [2]

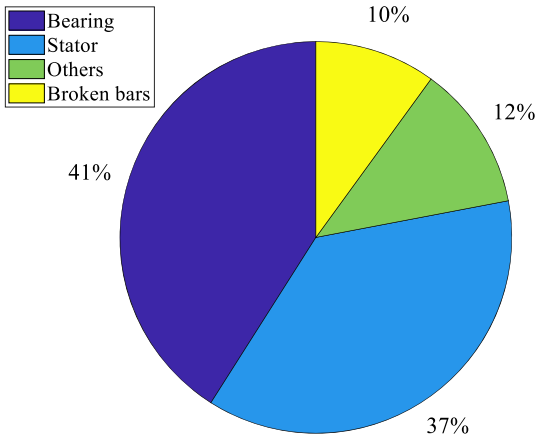

Fig. 2 Fault statistics on three-phase induction motors. Adapted from [26]

rotor the moving part. The stator is made up of thin magnetic ring-shaped steel plates with internal grooves where the windings are housed. The rotor is also composed of thin sheets of magnetic steel and with the longitudinally housed windings [24].

Figure 2 identifies the percentage associated with the main components of the motor in the total recorded failures in the industry [26]. This chart helps to understand the main causes of failure in three-phase induction motors and, therefore, will be studied further in the course of this work.

Bearing is a device that allows controlled relative movement between two or more parts. It serves to replace the sliding friction between the shaft and bearing surfaces with a bearing friction. The bearing is basically made up of two rings that have a track where the rotating elements rotate, attached to a cage. There are several causes of bearing failures. In addition to the normal failure process, that is, the appearance of small cracks below the raceway surface and bearing elements, there are other external conditions that cause a reduction in the bearing's lifetime, the main ones being [24]:

- *Contamination* The process of contamination occurs through small particles of varying hardness and abrasive nature which often contaminate the lubrication winding.
- *Corrosion* The corrosion process is initiated by the presence of water, acid, deteriorated lubrication, etc. As the corrosion process advances, particles are expelled resulting in the same abrasive action as contamination.
- *Improper Lubrication* Missing or excess lubrication causes the bearing elements not to rotate properly in the oil film, causing heating. This heating deteriorates the lubricant, accelerating the failure process.

- *Installation Problems* Failures originated by improper installation are caused by forcing the bearing against the shaft or housing, resulting in physical damage to the bearing. Other common problems generated by incorrect installations are: misalignment, shaft deflection, inner race warp and outer race warp.

In addition, possible rotor breakdowns include the development of rotor bar fractures, particularly in the region of short rings. This type of failure is 35% of all failures in the rotor as shown in Fig. 3.

Based on the above, this study will focus on the use of vibration analysis techniques, directed to predictive maintenance in induction motors. The main faults found in this type of motor are bearing failures and broken bar, also stands out the mechanical unbalance, which can most often be the root cause of another type of failure. Since these three types of failures are the most common, the failures will be studied and experienced in this work.

3 Artificial neural networks

The ability to learn by example is an important tool of human intelligence that arouse researchers in artificial intelligence, statistics, cognitive science and other related studies. Algorithms that can inductively learn from examples have been used to solve real-world problems [1].

The artificial neural networks (ANN) can be defined as a machine that is designed to model the way in which the brain performs a particular task or function of interest; the network is usually implemented using electronic components or simulated by digital programming. To achieve good performance, neural networks employ a massive interconnection of simple computational cells called neurons or processing units [15].

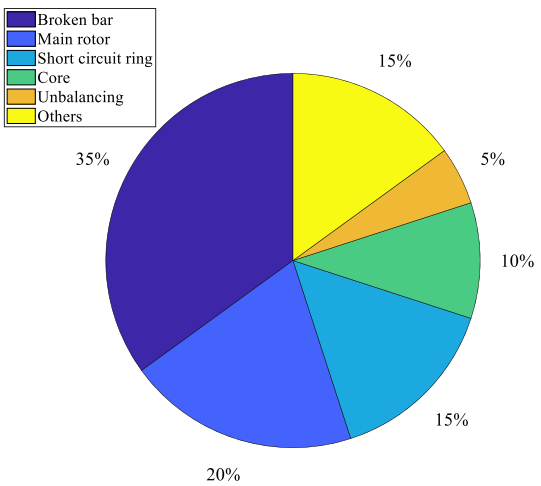

Fig. 3 Three-phase induction motors rotor failure statistics. Adapted from [24]

These systems are composed of several simple units (the artificial neurons) that are properly linked to achieve complex behaviors. Behavior is determined by the structure of the connections (topology) between neurons and the values of the connections (synaptic weights) [15].

3.1 ANN structure

The ability of humans to perform complex tasks and especially their ability to learn comes from the parallel and distributed processing of the brain's network of neurons. The neurons in the cortex, the outer layer of the brain, are responsible for the cognitive. A new experience or learning can lead to changes in brain structures. Such changes are realized through a rearrangement of neuron networks, reinforcing or hindering some synapses [15]. Figure 4 is a simplification of a model of artificial neuron.

This model consists of three basic elements: a set of n input connections (X_1, X_2, …, X_n) characterized by synaptic weights (W_{i1}, W_{i2}, …, W_{in}); an adder to accumulate the input signals and an activation function that limits the permissible amplitude range of the output signal (Y_i) to a fixed value [9].

The behavior of connections between neurons is simulated by their weights, which may have negative or positive values, depending on whether the connections are inhibitory or excitatory. The effect of a signal derived from another neuron is determined by multiplying the value (intensity) of the received signal by the weight of the corresponding connection ($X_i \cdot W_i$). The sum of the values of all $X_i \cdot W_i$ connections is performed, and the resulting value is sent to the activation function, which defines the output (Y_i) of the neuron [9].

In a simplified form, one artificial neural network can be seen as a graph where the nodes are neurons and the links are the function of synapses, as shown in Fig. 5.

In an ANN's full structure, the main parameters of the network are: the number of neuron layers, the number of neurons per layer, the types of connections between neurons and the degree of connectivity between neurons.

3.2 The learning process

The learning process of an ANN requires examples of real (or simulated/numerical) data. The interaction between data and an ANN is given by learning paradigms [19]. Two basic classes of learning paradigms can be considered: supervised learning and unsupervised learning [15].

- *Supervised learning* In this type of learning, examples are presented for the network and the network response

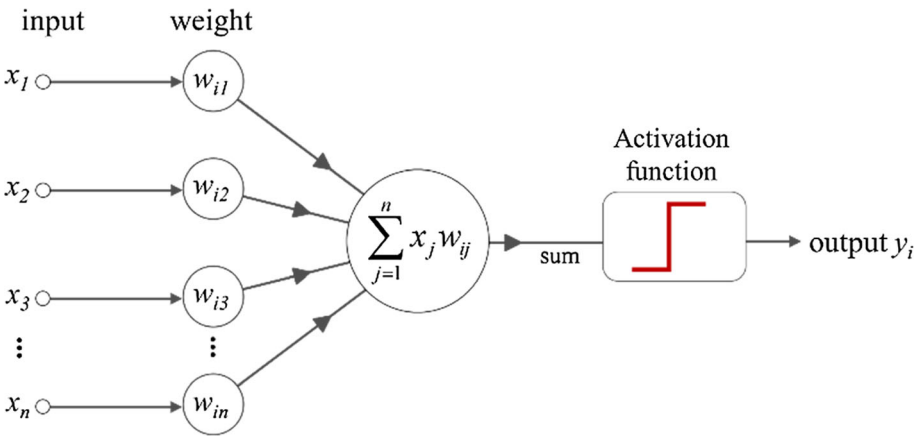

Fig. 4 Simplified representation of an artificial neuron

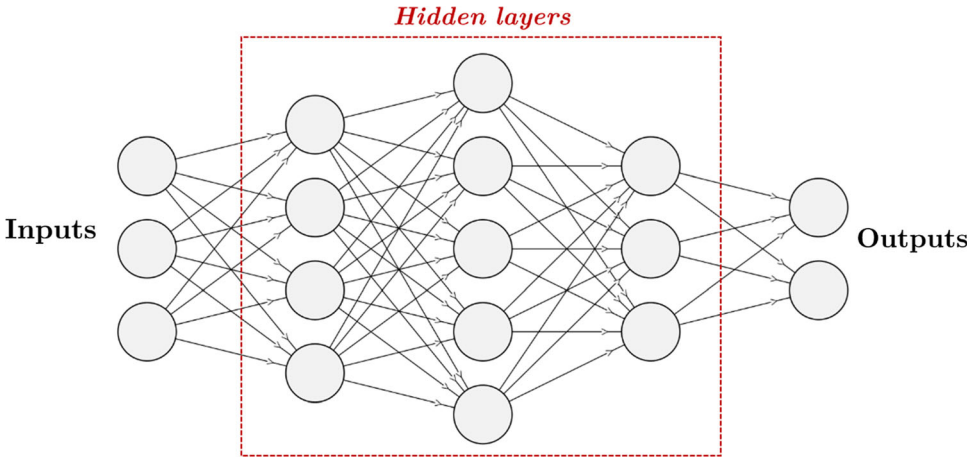

Fig. 5 Simplified representation of the artificial neural network

is evaluated against the desired response. The difference between the two responses, known as the error signal, is used to adjust the synaptic weights of the network. This procedure is performed step by step until the network responds correctly within a statistical sense [15].

- *Unsupervised learning* In this type of learning, the learning algorithms don't want the knowledge of the desired outputs, that is, not using examples of input and output to be learned by the network. The ANN self-organizing [15].

For a good ANN configuration, you should define a model that is not too rigid to not faithfully model the data, but, on the other hand, not so flexible as to model the noise in the data.

3.3 Choose criteria for ANN

This is not a general rule, but below are parameters that help in choosing the structure of the ANN.

3.3.1 Number of hidden layers

After study, it was observed that a large number of hidden layers is not recommended, as each time the average error during training is used to update the weights of the immediately preceding layer, it becomes less accurate. Only the output layer has a more accurate sense of the error made by the network. The last hidden layer receives an estimate of the error and the second to last hidden layer receives an estimate of the estimate, and so on. Empirical testing does not show great advantages in using two or more hidden layers for minor problems. Therefore, for most problems only one hidden layer is used and at most two, for example, in case of function approximation problems [7].

3.3.2 Number of neurons in hidden layer

Its definition is empirical, but care must be taken not to use too many units leading the network to memorize training data (overfitting) rather than extracting the general characteristics that will allow a good generalization. On the other hand, using a few units of neurons can force the

network to spend a lot of time trying to find an optimal representation [7].

There are some proposals on how to determine the number of neurons in the hidden layers of an ANN and the most used are:

- Define the number of neurons according to the input and output layers of the network, for example, the arithmetic mean between input size and output size [19].
- Use the number of synapses ten times less than the number of training patterns. If the number of patterns is much larger than the number of synapses, the network does not converge during training [7].

3.3.3 Learning rate and momentum

A very low learning rate makes learning the network very slow, and if it is too high it causes training swings and prevents convergence. Usually its value ranges between 0.1 and 1.0. Some programs have this adaptive value, so choosing an initial value is not a problem. However, for some programs this value is fixed and should not be too high [7].

In addition, backpropagation learning can be speeded up by using correct values of momentum. The value of the learning rate can also influence whether the network achieves a stable solution. If the learning rate value is too large, then the weight changes no longer approximate a gradient descent procedure.

As a matter of facts, using the largest learning rate possible without triggering oscillation is desirable. This would offer the most rapid learning and the least amount of time spent waiting at the computer for the network to train. One method that has been proposed is a slight modification of the backpropagation algorithm so that it includes a momentum term.

3.3.4 Training dynamics

The training dynamics can be divided into two main fronts:

- By default: Weights are updated after each training pattern has been submitted. The order of pattern presentation can be reorganized to speed up training [7].
- By *batch:* Weights are updated after all training standards have been submitted to the net. This technique is more stable and training is less influenced by the order in which patterns are presented to the network. But it becomes slow if the pattern set is large and redundant. Although requiring more memory compared to training by default, this type of training is more stable though slower [7].

3.3.5 Training stop criteria

The training stop criteria can be defined in many ways, for example:

- By number of seasons: This is the number of times the pattern set is presented to the network. Too many seasons can cause the network to lose its generalizing power. But a very small number of times may not reach its performance [7].
- By error: Training state is terminated after the mean square error falls below a predefined value (e.g., 10^{-6}). This value should be adjusted according to the performance of the network result. It is important to note that a small value does not necessarily imply good generalization [7].
- Validation: Training is interrupted every n epochs and a network error estimation is performed on the test dataset. From the moment, the measured error in the test set goes up, the training is terminated. Thus, we seek to know the exact moment when the network begins to lose generalization [7].

4 Experimental methodology

This section will discuss all the details and methods used to perform the controlled vibration experiment. In summary, there are motors with four known different operating conditions and a classification is realized through vibration signal analysis.

In order to create and analyze the motor defects (fault condition), two approaches have been adopted. For the initial vibration response analysis, the experimental design was based on the design of experiments (DOE) methodology, which is a statistical technique capable of modeling and optimizing experiments. This technique is a technique consolidated in the literature [3, 4, 20]. The first involves the use of the motors until their failure, where the entire process is monitored and changes in time can be analyzed. As it is a lengthy process, failure is usually accelerated. In the second approach, defects are artificially created, so it is possible to compare with machines under normal operating conditions. In this study, the second approach is adopted considering induced faults.

4.1 Experimental setup

All tests were conducted at PS solutions. The bench comprises eight-motor used AC induction of 0.5 CV directly coupled to a 6-blade fan (Fig. 6). Motor nameplate data are in Table 2.

Fig. 6 Motor marathon

Table 2 Marathon motor plate data

	$f = 60$ Hz	$f = 50$ Hz
Power (HP)	0.5	0.33
Rotation (rpm)	3450	2850
Voltage (V)	208–230/460	190/380
Amperage (A)	2.1–2.2/1.1	2.0/1.0
Service factor	1.15	1.15

Each pair of motor has a known operating condition, where:

- *Normal* refers to the motors in its full operating condition.
- *Hole Bearing* refers to the motor that has its bearing drilled to simulate defects such as cracks and/or deformations in the bearing (Fig. 7c).
- *Broken Bar* refers to a broken bar in the squirrel cage rotor. In large motors, this structure is welded and may break because it is a weak point (Fig. 7b).
- *Mechanical Unbalance* refers to an unbalance created through a bolt and a nut made in the center of one of the fan blades (Fig. 7a).

The vibration measurement was performed with a uniaxial accelerometer IMI (Fig. 8). The sensor has a frequency range of ± 3 dB (0.5 to 10,000 Hz), measuring range of ± 50 g (± 490 m/s), cross-sensitivity of $< 7\%$, sensitivity of 100 mV/g [10.2 mV/(m/s^2)] and resonant frequency in the order of 25 kHz. These characteristics make the sensor suitable for the monitored vibration intensity and frequency levels, since the motor mass is much larger than the accelerometer and the monitored vibration frequencies are low.

The accelerometer is fixed to the motor housing on the bearing bracket by means of a threaded previously installed (Fig. 8). In this position, the vibration signal is measured in the radial direction of the motor shaft.

4.2 Vibration signal and conversion system

The acquisition of the vibration signal is made by the system Preditor®, system developed and manufactured by PS Solutions. The Preditor® allows 24-bit sampling at a rate of 46,875 samples per second. The sampling time is approximately 6 s. The signal conversion is done by the software developed by PS solutions that comes with the Preditor® itself. It can display both the vibration signal and

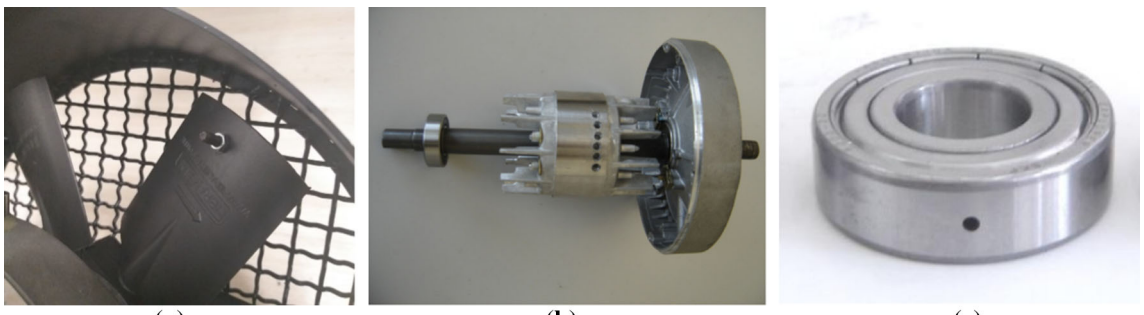

Fig. 7 Three different fault conditions: **a** unbalancing, **b** broken bar and **c** bearing

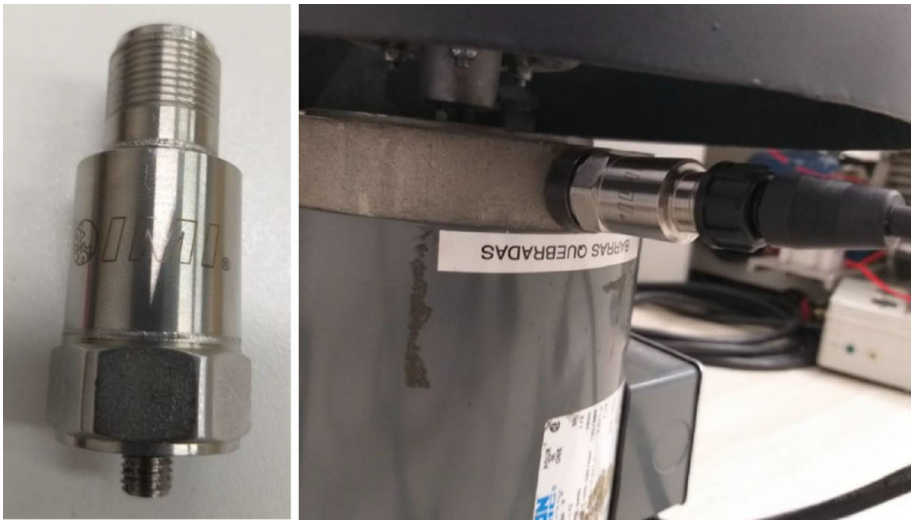

Fig. 8 IMI accelerometer and accelerometer coupling

export to a text file. In this work, we chose the option to export to text file due to the need to process the signal in the software MATLAB®.

The conditions during the experiment are simple: The motor is mains powered at 60 Hz, without frequency inverter or any kind of speed and torque control. This is done to simulate an actual operating condition and provides a stable condition for measurement. The vibration of each motor was measured individually so that there is no

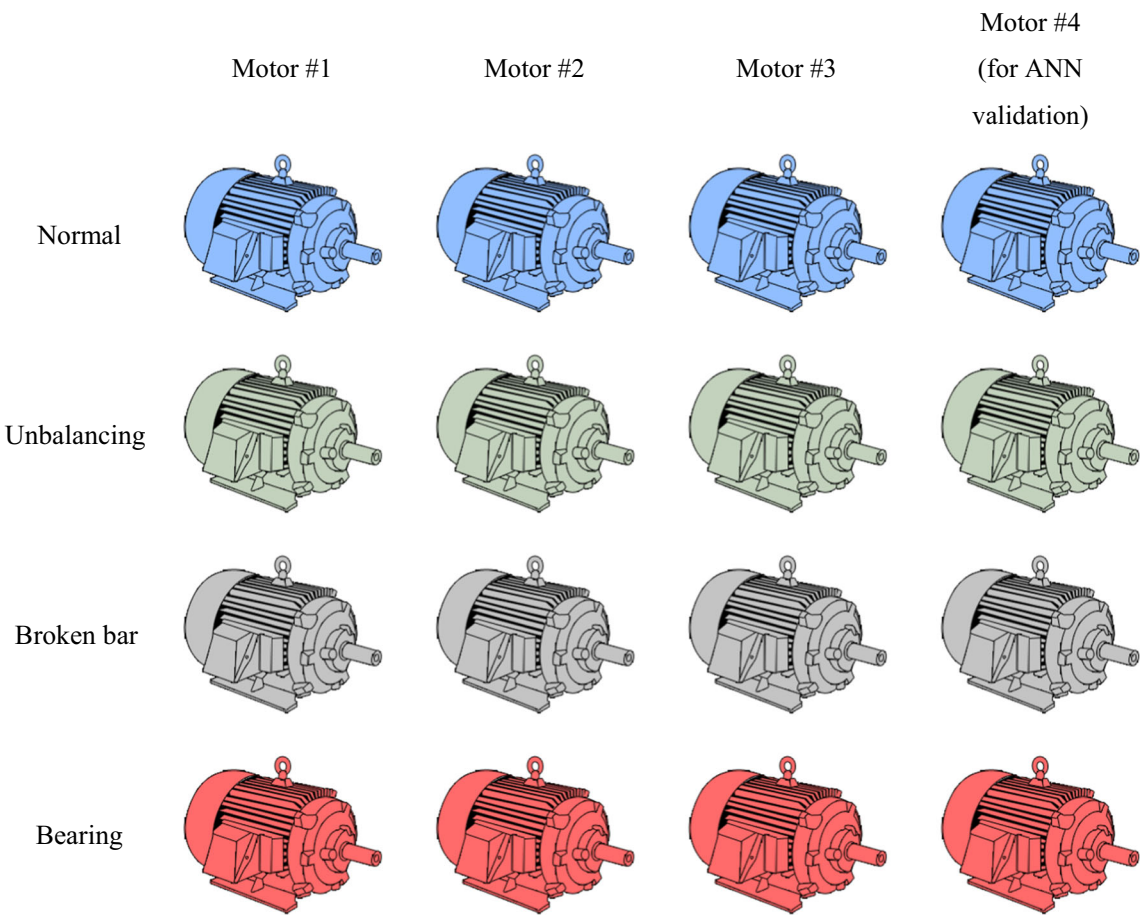

Fig. 9 Scheme of 16 motors, divided into four different operating conditions and four datasets: three for the ANN training and one for validation

interference from one motor to another. Each motor was measured twice, totaling 16 vibration signals (Fig. 9).

4.3 Neural network architecture

For the best possible results, it is extremely important to choose the style of neural network that best fits the type of problem. A wrong choice at this stage will likely result in failure to use the neural network. The software through the toolbox Neural Network Toolbox™ offers four different options of ANN, as follows: fitting, pattern recognition, clustering and time series. For the problem at hand, *pattern recognition* was chosen as the neural network style. It has also been chosen a feed-forward neural network. In this work, twelve vibration signals will be used for network training and the remaining four vibration signals for testing and validation of the neural network.

The choice of number of hidden layers depends on the complexity of the problem studied. For the problem at hand, the neural network will only classify the data based on the patterns reported in the training. Therefore, a high number of hidden layers are not required. Thus, only one hidden layer was chosen for neural network. The activation function of the hidden layer is a sigmoidal type. The ANN structure is intimately linked to used datasets, and in this study, a total of [20,4] neurons was chosen in the hidden layer.

Input and target data are organized into two matrices. The inputs matrix is formed by vectors that contain the vibration signal data of the first 3 measurement sets, and the *targets* matrix is also formed by *target* vectors (**T**), where **T** = [Normal, Broken Bar, Bearing, Mechanical Unbalance]. If **T** = [1 0 0 0], we have the normal operating condition, if **T** = [0 1 0 0], we have a broken bar condition, if **T** = [0 0 1 0], we have if the bearing failure condition and if **T** = [0 0 0 1], then there is the mechanical unbalance condition. Equation 1 best exemplifies the targets matrix used for neural network training. As stated in previous sections, backpropagation learning can be speeded up by using correct values of momentum. In this study, a momentum value of 0.90 was used.

$$\text{output } [\mathrm{O}] = [\{\mathrm{O_N}\} \quad \{\mathrm{O_{BB}}\} \quad \{\mathrm{O_{Be}}\} \quad \{\mathrm{O_U}\}] = \begin{bmatrix} 1 & 0 & 0 & 0 \\ 0 & 1 & 0 & 0 \\ 0 & 0 & 1 & 0 \\ 0 & 0 & 0 & 1 \end{bmatrix} \tag{1}$$

where: $\{\mathrm{O\text{-}_N}\} = \{1\ 0\ 0\ 0\}^{\mathrm{T}}$, $\{\mathrm{O\text{-}_{BB}}\} = \{0\ 1\ 0\ 0\}^{\mathrm{T}}$, $\{\mathrm{O\text{-}_{Be}}\} = \{0\ 0\ 1\ 0\}^{\mathrm{T}}$, $\{\mathrm{O\text{-}_U}\} = \{0\ 0\ 0\ 1\}^{\mathrm{T}}$ are the output for the conditions normal, broken bar, bearing and unbalance, respectively.

A first attempt was to use the FFT of vibration signals as *input* to the neural network, but this deal was prohibitive given the excessive number of data, about 260 thousand points per signal, these excess data confused the neural network and the same that failed to come up with a converged solution. Thus, a different approach to the *inputs* had to be adopted, and this solution should extract from the "pure" signal information that characterizes it in a condensed way. After a literature review on the subject, we came to the conclusion that using statistical parameters to extract signal key information is the best way to solve the problem.

According to Patel and Upadhyay [22] and Gaud et al. [11], the best statistical parameters to characterize motor damage through the vibration signal are: RMS, Peak, Skewness, Kurtosis, Mean and Crest Factor.

Root Mean Square (RMS)

The RMS is defined as the square root of the mean of the sum of squares of the sampled signal. Its formula is given by Eq. 2.

$$I_1 = \mathrm{RMS} = \sqrt{\frac{1}{N}\sum_{k=1}^{N}(a_k - \bar{a})^2} \tag{2}$$

where N = number of samples k = sample index a_k = index sample k and a = mean of samples

Peak

The *Peak* marks the largest value found in the vibration signal. It is calculated by her Eq. 3.

$$I_2 = \mathrm{Peak} = \max(a_k) \tag{3}$$

Skewness

This is the third-order moment over your average. This measures the asymmetry of the data distribution. Its formula is given by Eq. 4.

$$I_3 = \mathrm{Skewness} = \frac{1}{N}\sum_{i=1}^{N}\left[\frac{x_i - \mu}{\sigma}\right]^2 \tag{4}$$

where i = sample index a, x_i = the index, μ = mean of samples and σ = standard variation of samples

Kurtosis

It is the fourth-order moment normalized by the square of variance of a signal. It is a measure that characterizes the "flattening" of the normal curve. It is calculated by her Eq. 5.

$$I_4 = \mathrm{Kurtosis} = \frac{\frac{1}{N}\sum_{k=1}^{N}(a_k - \bar{a})^4}{a_{\mathrm{RMS}}^4} \tag{5}$$

Mean (μ)

These are the average values of a signal in the time domain. It indicates the central tendency of this database. Its formula is given by Eq. 6.

$$I_5 = \text{Mean} = \mu = \frac{\sum a_k}{N} \tag{6}$$

Crest factor (CF)

The *Crest factor* indicates how extreme the peaks are in a waveform. It is calculated by her Eq. 7.

$$I_6 = \text{Crest Factor} = \frac{a_{\text{peak}}}{a_{\text{RMS}}} \tag{7}$$

In short, the created neural network collects the pure vibration signal data, extracts the important information from these signals through the six equations mentioned above. With these results and targets defined, the neural network will place weights on the equations to better rank them among the four possible targets.

5 Results

5.1 Results of vibration analyses

In this section, we discuss the results obtained by vibration analysis. It will be made to analyze for a dataset, that is, a motor vibration signal in the condition typical one bearing bore with vibration signal, a vibration signal of the mechanical unbalance and vibration signal of the broken bar.

Figure 10 shows the acceleration vibration signals acquired under all four motors operating conditions for the first motor group. It can be seen that the signal itself is very similar, except that the amplitude is higher at bearing fault and lower at normal operating condition.

By analyzing the amplitude of the vibration signals over time, it is clear that the amplitude of the bearing signal is large (i.e., highest amplitude level) compared to the normal motor signal, confirming the sensitivity and effectiveness

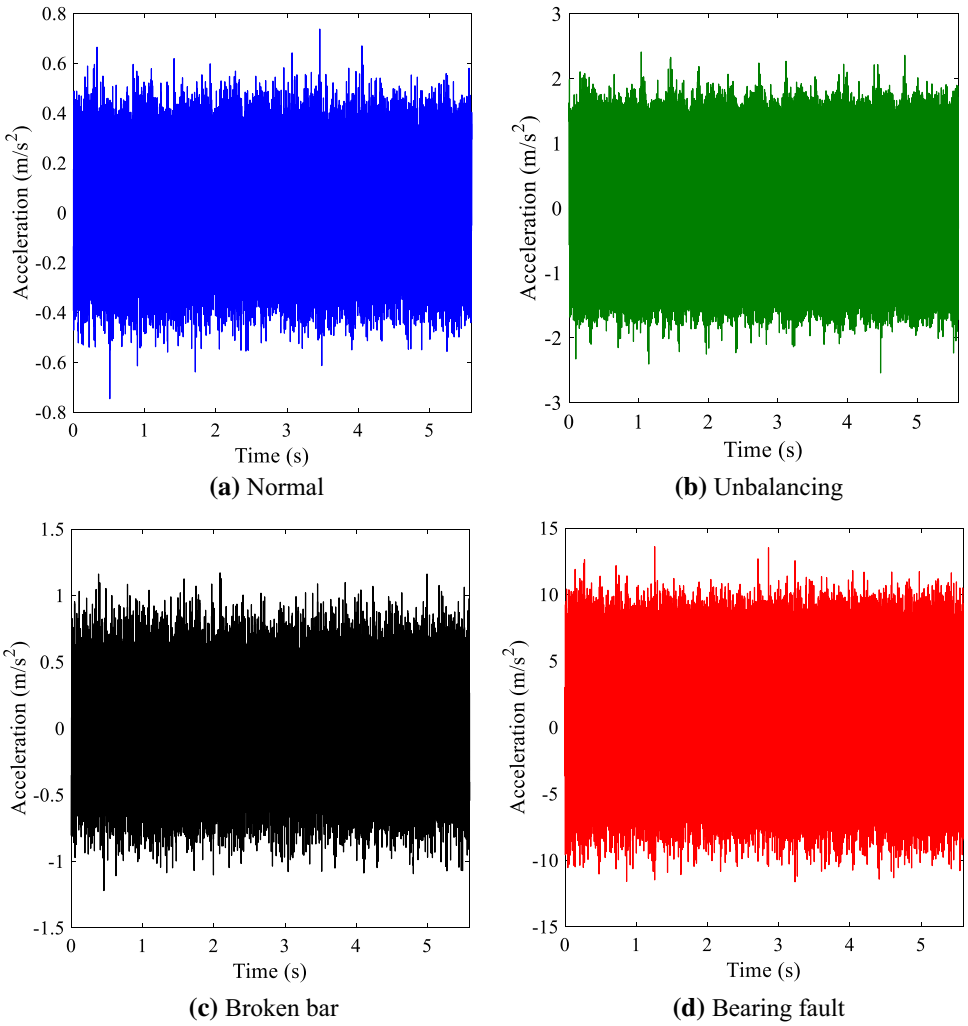

Fig. 10 Time domain vibration signal for the four operating conditions of the electric motor

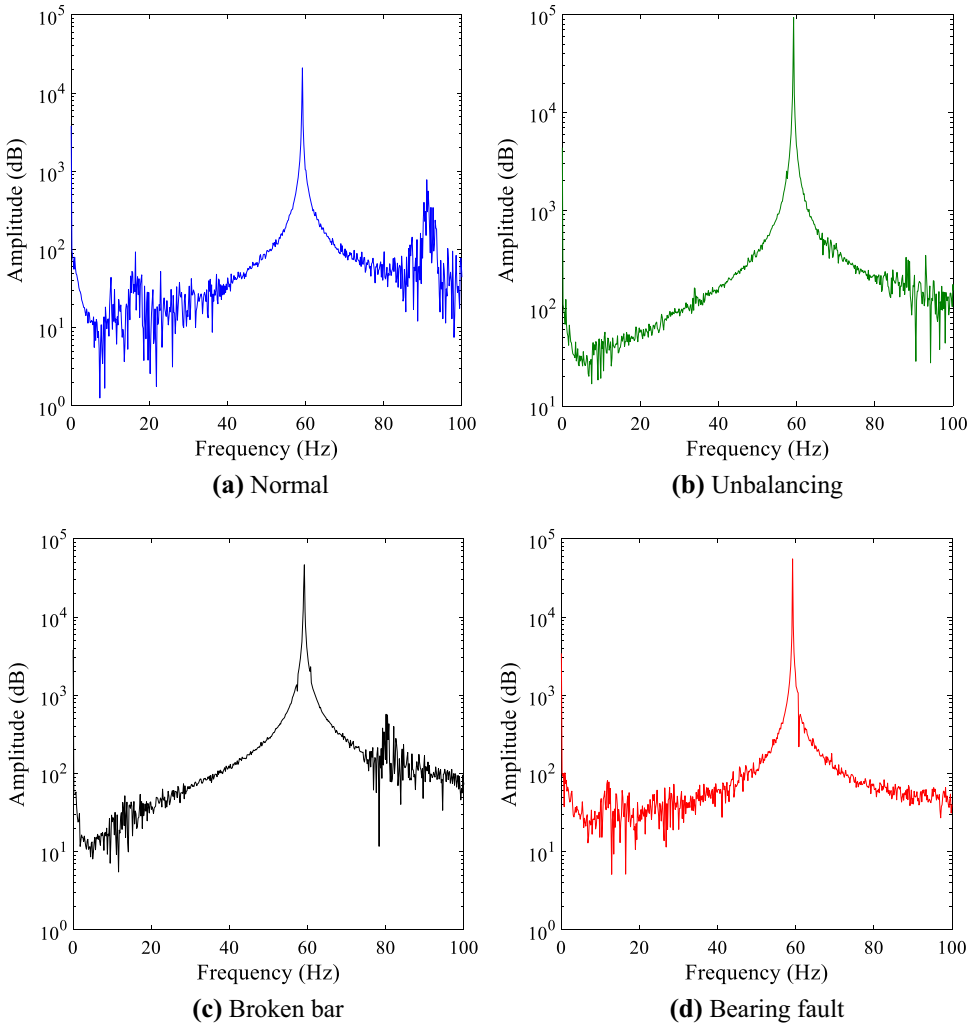

Fig. 11 Frequency spectrum of motors in each operating condition

of vibration analysis for bearing fault detection. For the mechanical unbalance and broken bars, there is a considerable increase in the amplitude of vibration, but only with the signal in time cannot be concluded whether the vibration is adequate or not to detect the failure.

In addition, Fig. 10 shows vibration signals acquired with a high sampling frequency, having more than 200 thousand points. Using a data vector of this size would be prohibitive in neural network training. An alternative is to analyze the vibration response in the time domain. Figure 11 shows the frequency domain response for the four operating conditions. It can be concluded that the inserted defects did not change the motor operating frequency ($\sim$ 59.8 Hz).

Analyzing the frequency spectrum, it can be seen that the motor operating frequency is close to 60 Hz, that is, all defects are in the early stage and are not about to cause the motor to stop as a whole. Additional analysis revealed that new amplitude peaks, at 547.9 Hz and 236.6 Hz, for the bearing and unbalancing signals. These peaks reinforce the effectiveness of bearing fault detection and the effectiveness of mechanical unbalance fault analysis, given that they have the same peaks in all signals. For the broken bar signal there is no frequency peak, so to prove the effectiveness of vibration analysis to detect this type of failure another type of transform should be used or simply vibration is not the most appropriate method.

5.2 Fault condition effects on the vibration responses

As mentioned earlier, the pure vibration signal is inconvenient when treated as input to the neural network. For this, we chose to extract information from this signal (vector) that could add more information quality and sensitivity due to the evaluated failure. Figure 12 shows as an example the six responses (inputs I_1 to I_6) evaluated, which are statistical information of the signal.

In order to verify the behavior of the response distributions and the central tendency for each type of analysis, a

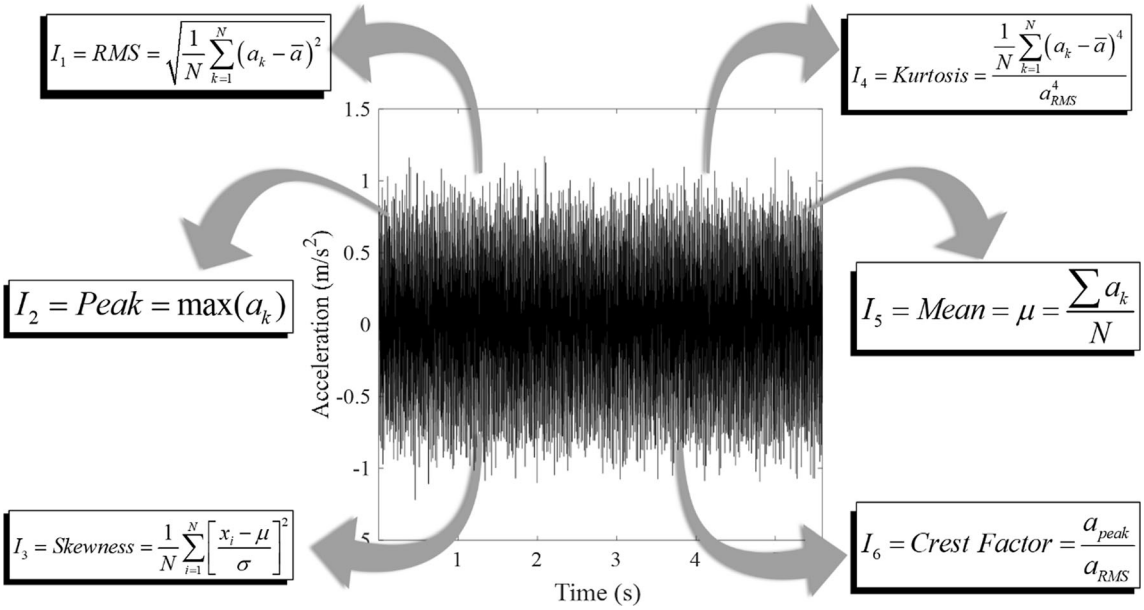

Fig. 12 Data extracted from the time domain vibration signal

boxplot was created, as shown in Fig. 13. This graph allows to verify the descriptive statistics information, where it is possible to verify that the values for mean showed the lowest variability for all failure modes. The RMS data present low-data discrepancy, analyzing individually, but with different averages, mainly for the bearing model. In skewness, the average values are very close; however, the bearing model presented a higher level of dispersion, compared to the others in this type of analysis. For the analyses of Kurtosis and Crest Factor, a similar behavior was verified in the average values; however, the latter presented greater variability in the data distributions. Finally, checking the peak analysis has low variability for broken bar and normal modes, followed by greater variability (especially in the first quartile) for unbalance failure mode. In addition, in this analysis it is possible to verify a distribution behavior that indicates a high variability in bearing mode, inferring a higher instability compared to other modes, both of the same type of analysis as in the others. It is important to highlight that none of the modes in all analyzes presented outlier values.

Equally important, after verifying the variability of the fault condition for each type of analysis, the relationship between the response and the respective predictors can also be evaluated. For this, one can use the main effects graphs, considering a confidence interval (CI) of 95%, illustrated in Fig. 14. It is possible to verify that Fig. 14a and b shows behavior main effects, where the broken bar failure mode is related to the lowest condition analyzed for both cases and closest to the ideal condition, which is called normal. In the skewness analysis (Fig. 14c), bearing failure mode has a high value for the condition, but with behavior closer to the normal condition. The same is verified for mean analysis (Fig. 14e), but with higher values found for these conditions. Regarding Fig. 14d, it can be inferred that the main effect for Kurtosis analysis indicates that the Unbalance failure mode exhibited the same behavior as the normal condition. Finally, Fig. 14f indicates a distinct behavior, where bearing and unbalance failure modes behave closer to normal condition; however, one of them is related to the higher value, while another is related to a lower value than the ideal condition, respectively. It is important to notice that according to Table 7 ("Appendix"), only the responses RSM, Peak and Kurtosis present a level of significance of the main effect considering an interval of 95%. However, this does not restrict its inclusion in the proposed method. It just indicates that it is not possible to reach conclusions regarding the main effects.

5.3 ANN's results

This section describes the results obtained by the artificial neural network in two parts: The first presents the results obtained with the training of the neural network, mainly in the form of graphs. The second presents the validation and testing of the neural network. A summary of the neural network can be seen in Fig. 15.

As stated earlier, the "pure" vibration signal is prohibitive to the neural network. Thus, statistical data were used to extract important information to characterize a vibration signal. Table 3 is the result of RMS, Peak, Skewness, Kurtosis, Mean and Crest Factor for the 12 signals used for neural network feeding.

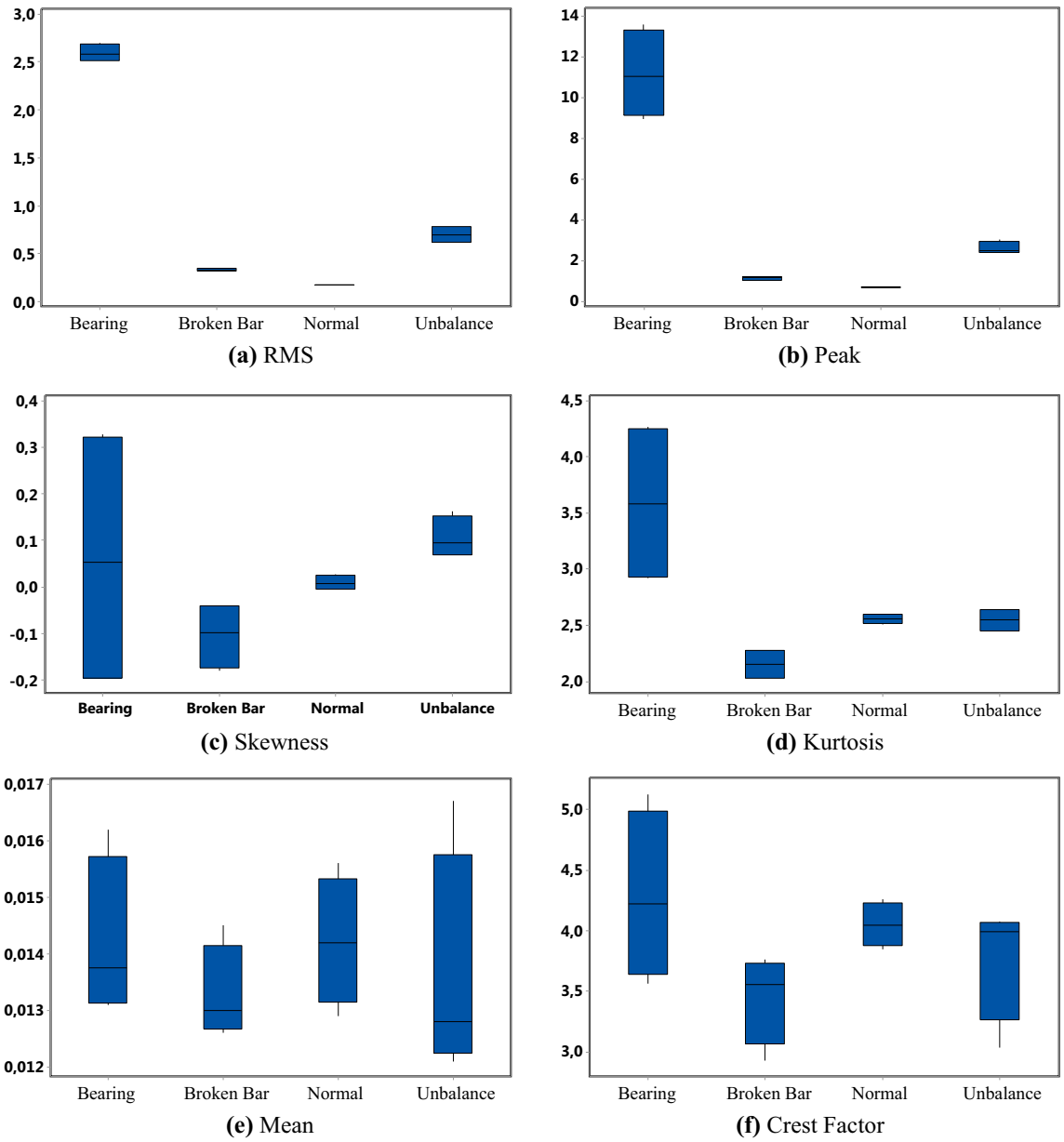

Fig. 13 Boxplot for all the six evaluated input data for sixteen motors

5.3.1 ANN training results

Network performance is measured by the mean square error. Figure 16 shows the evolution of the network during training. *Epoch* in this case means the amount of iterations performed by the neural network. The mean square error (MSE) results translate the network performance function. It measures the network's performance according to the mean of squared errors. The MSE algorithm is an example of supervised training, in which the learning rule is provided with a set of examples of desired network behavior and can be calculated as shown in Eq. 8.

$$\mathrm{MSE} = \frac{1}{Q}\sum_{k=1}^{Q} e(k)^2 = \frac{1}{Q}\sum_{k=1}^{Q} [t(k) - \alpha(k)]^2 \tag{8}$$

where t is the corresponding target output and α is the network output. As each input is applied to the network, the network output is compared to the target. The error (e) is calculated as the difference between the target output and the network output. The goal is to minimize the average of the sum of these errors [6].

In addition, the confusion matrix shows the amounts of correct and incorrect classifications. The correct ratings are the green frames in the diagonal matrix; the red frames are the incorrect ratings.

(Intentionally left blank)

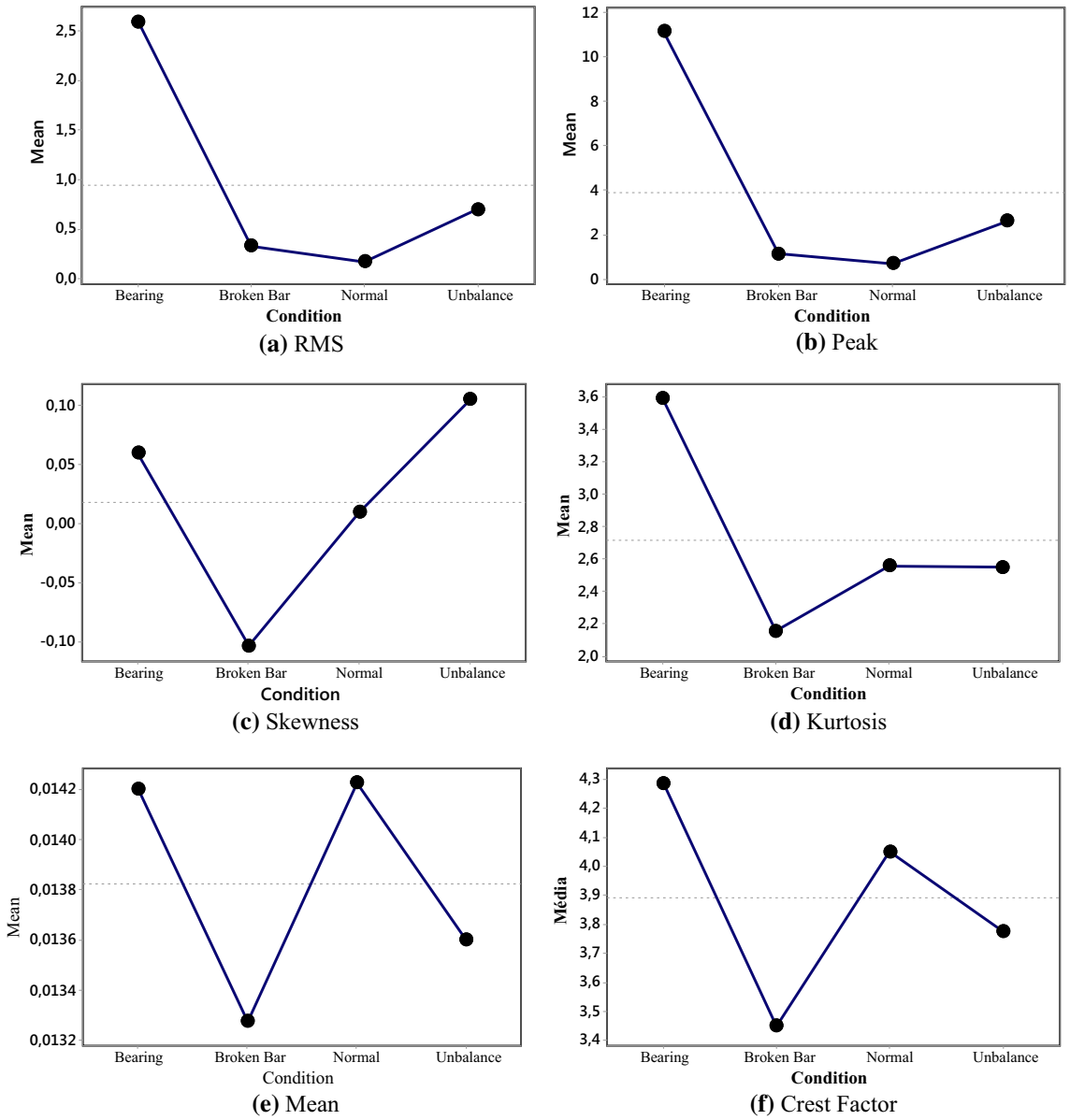

Fig. 14 Mean of the main effects for all the six evaluated input data for sixteen motors

The confusion matrix, **C**, can be derived from the outer product of the transpose of the target matrix, **T** and the output matrix, **Y**, as shown in Eq. 9 [16].

$$\mathrm{C} = \mathrm{T}^{T}\mathrm{Y} = \begin{bmatrix} \sum_{k=1}^{m} t_{k1}y_{k1} & \sum_{k=1}^{m} t_{k1}y_{k2} & \cdots & \sum_{k=1}^{m} t_{k1}y_{kc} \\ \sum_{k=1}^{m} t_{k2}y_{k1} & \sum_{k=1}^{m} t_{k2}y_{k2} & & \sum_{k=1}^{m} t_{k2}y_{kc} \\ \vdots & & \ddots & \vdots \\ \sum_{k=1}^{m} t_{kc}y_{k1} & \sum_{k=1}^{m} t_{kc}y_{k2} & & \sum_{k=1}^{m} t_{kc}y_{kc} \end{bmatrix} \quad (9)$$

If the neural network has been well trained, the percentage of misclassifications is very small, otherwise it is recommended to change the number of neurons in the hidden layer or even add another hidden layer. Figure 17 shows the neural network's confusion matrix. The neural network classified all data correctly, which reinforces that the adopted parameters were correct.

The receiver operating characteristic (ROC) shows the relationship between true positive and false positive. ROC characteristic is a metric used to check the quality of classifiers.

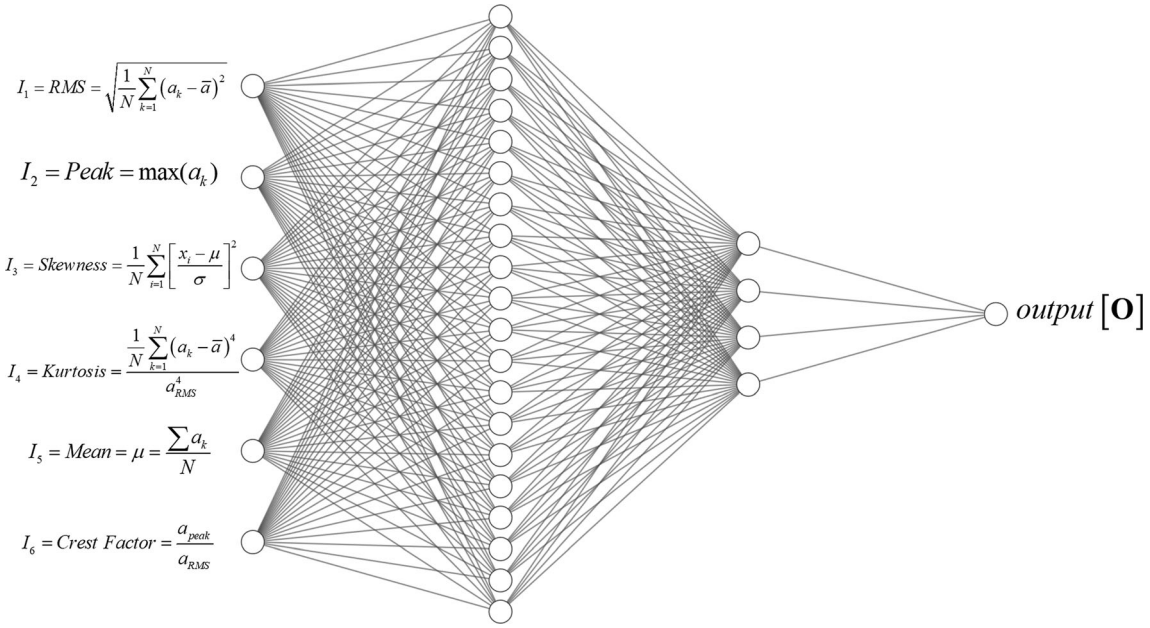

Fig. 15 Artificial neural network architecture considering 6 input, 20/4 neurons in hidden layer and 1 output

Table 3 Neural network inputs for the training stage considering three dataset

Condition	RMS	Peak	Skewness	Kurtosis	Mean	Crest factor
Normal (M1)	0.173	0.7372	− 0.0019	2.5793	0.0145	4.2622
Normal (M2)	0.1717	0.7078	0.0186	2.5078	0.0156	4.1225
Normal (M3)	0.1725	0.664	− 0.0056	2.6042	0.0129	3,8487
Broken bar (M1)	0.3217	1.1703	− 0.0433	2.2784	0.0131	3.6372
Broken bar (M2)	0.3437	1.1931	− 0.1787	2.039	0.0145	3.4715
Broken bar (M3)	0.3191	1,2002	− 0.0392	2.2738	0.0126	3.7608
Bearing (M1)	2.6521	13,6032	0.2983	4,2641	0.0131	5,1292
Bearing (M2)	2.5098	8.9542	− 0.1926	2.9662	0.0162	3.5677
Bearing (M3)	2669	12,367	0.3289	4.2058	0.0132	4.582
Unbalance (M1)	0.7937	2,4119	0.1628	2,4491	0.0167	3.0389
Unbalance (M2)	0.6333	2.5835	0.0694	2.6419	0.0127	4.0793
Unbalance (M3)	0.7558	3.0452	0.1292	2,4598	0.0121	4.0292

The ROC curve is a performance measurement for classification problem at various thresholds settings and also represents degree or measure of separability. It tells how much model is capable of distinguishing between classes. The ROC curve is plotted with true positive rate (TPR) (Eq. 10) against the false positive rate (FPR) (Eq. 11).

$$\mathrm{TPR} = \frac{\mathrm{TP}}{\mathrm{TP} + \mathrm{FN}} \tag{10}$$

$$\mathrm{FPR} = \frac{\mathrm{FP}}{\mathrm{TN} + \mathrm{FP}} \tag{11}$$

where TP is the true positives, FN false negatives and FP are the false positives.

The best classifiers will have a line from bottom left to top left and top left to top right. Figure 18 shows the ROC neural network created. From this curve, it is clear that the neural network has classified all data correctly, with no false positives.

The error histogram (error histogram) shows the error between the target value and the value found by the neural network after training. The more concentrated the histogram is near zero error (consider scale), the better the neural network is trained. Figure 19 shows the error histogram of the trained neural network.

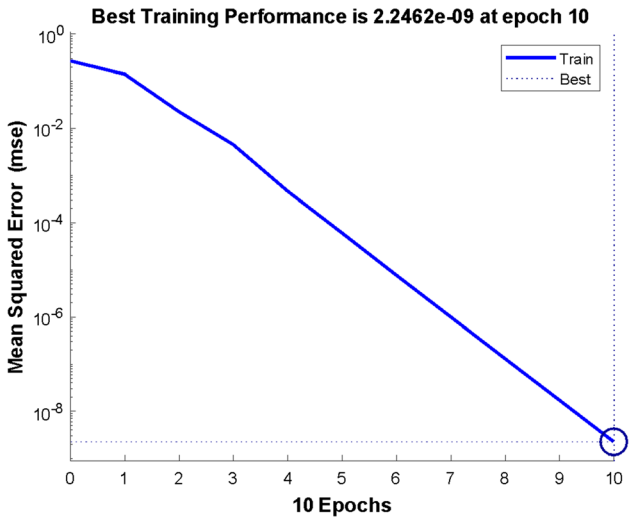

Fig. 16 Best training perfomance

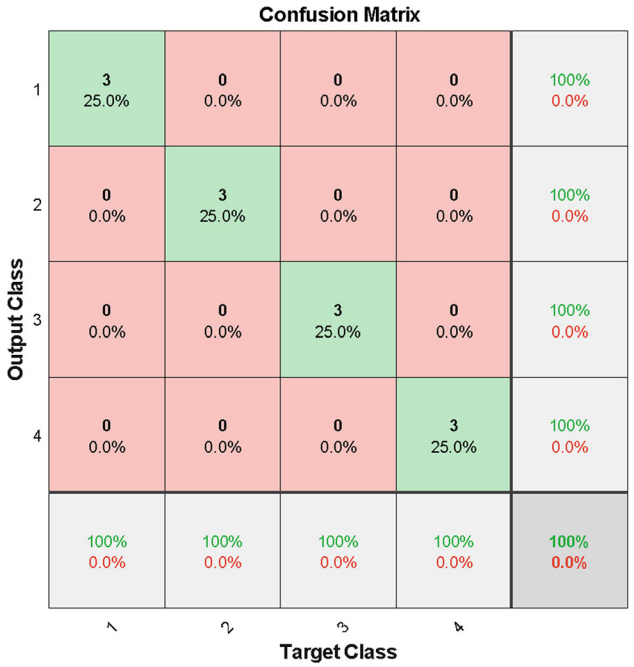

Fig. 17 Confusion matrix

5.3.2 ANN test and validation

To perform the validation of the ANN was used the four remaining vibration signals with previously stated. These data are unknown to the neural network, so it will be possible to assess whether the Neural Network is really well trained. To validate the neural network, tests were performed, one to determine if the neural network is consistent with itself and another to assess if it can classify the four operating conditions correctly. In the first test, the neural network was feed with four equal vibration signals (Table 4) from a motor under normal condition and the

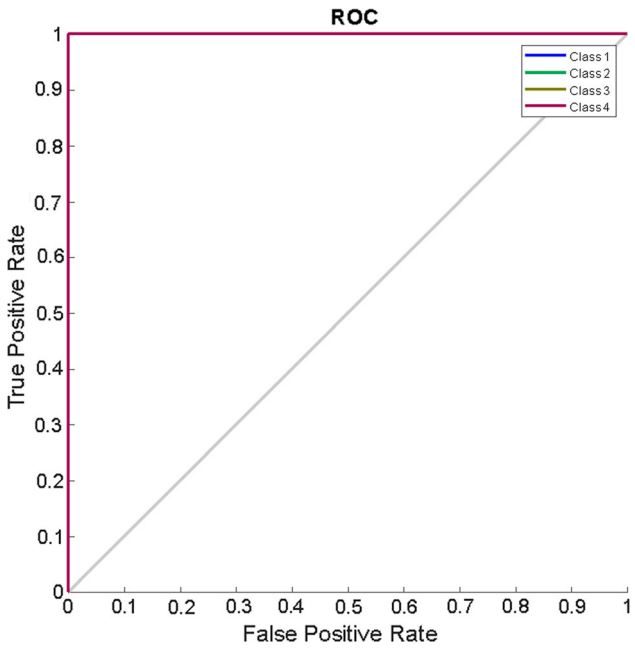

Fig. 18 Reciver operating characteristic (ROC)

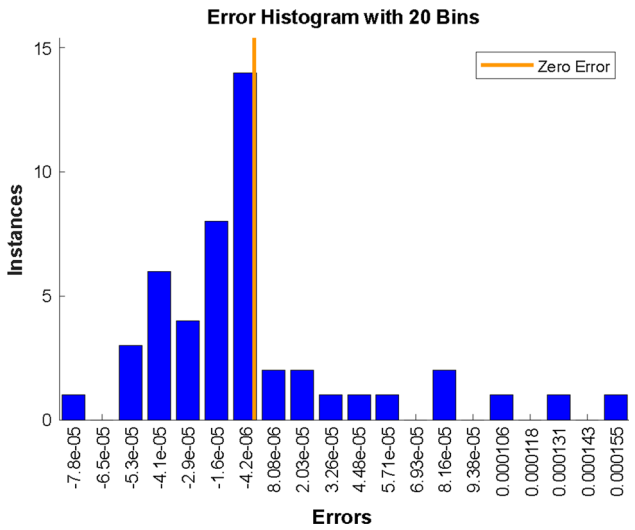

Fig. 19 Error histogram

ANN was able to correctly and coherently classify the motor operating condition. In the second test, the neural network was fed with four different vibration signals (mechanical, normal, broken bar, bearing). The results are presented in Table 5.

Also, for this test, the neural network was able to correctly classify the motor operating condition. A final test was also performed to validate that the network will not misclassify a signal of an operating condition for which it has not been trained. In fact, good ANN classification results are not expected when using data outside the training phase. On the other hand, in the particular problem

Table 4 Neural network inputs for the validation stage considering the last dataset of motors #4

Condition	RMS	Peak	Skewness	Kurtosis	Mean	Crest factor
Normal (M4)	0.1718	0.6818	0.0267	2.5417	0.0139	3.9670
Broken Bar (M4)	0.3744	1.0175	− 0.1543	2.0290	0.0129	2.9261
Bearing (M4)	2.5166	9.7325	− 0.1967	2.9224	0.0143	3.8673
Unbalance (M4)	0.0610	2.4163	0.0696	2.6382	0.0129	3.9569

Table 5 Rating validation

Defect type	Unbalance	Normal	Broken bar	Bearing
Target [**T**]	0	**1**	0	0
	0	0	**1**	0
	0	0	0	**1**
	1	0	0	0
Output [**O**]	0.0000	**0.9998**	0.0000	0.0000
	0.0000	0.0000	**1.0000**	0.0001
	0.0000	0.0000	0.0000	**0.9999**
	1.0000	0.0002	0.0000	0.0000

Bold values are indicate the output vector

of this study, the vibration response in the time domain for electrical unbalance (Fig. 10c) is very similar to the case of the broken bar (Fig. 20a). This type of situation could generate a false positive classification, that is, if the ANN is not properly trained, it would classify the electrical unbalance condition as a broken bar.

Thus, the same motor was taken with an unknown fault in the network, in this case an electrical unbalance condition, caused by a short circuit in one of the turns of the motor. The electrical fault (unbalance) was carried out by means of a cut in the internal turns of the motor, which certainly causes deterioration in the operation of the motor. This signal was also processed equally to all previous signals and fed to the neural network. The result is presented in Table 6. Equation 8 shows the output result of neural network fed with vibration signal of electric unbalance.

$$\text{output } [\text{O}] = \begin{Bmatrix} 0 \\ 0.8858 \\ 0.1060 \\ 0.0082 \end{Bmatrix} \tag{8}$$

For the signal of electrical unbalance, it was clear that the network could not classify the signal as another condition, since no value has come relatively close to 1. Thus, it is concluded that the neural network is not biased allowing a robust classification.

The results of the vibration analysis prove the effectiveness of this method to detect faults in electric motors, mainly faults of mechanical origin. In this case, the defects were already known, but if they are not, by analyzing vibration, bearing, mechanical unbalance defects are easily identified by analyzing their FFT's. The broken bar defect is already a little more difficult to detect since its amplitude is not as large as the other defects.

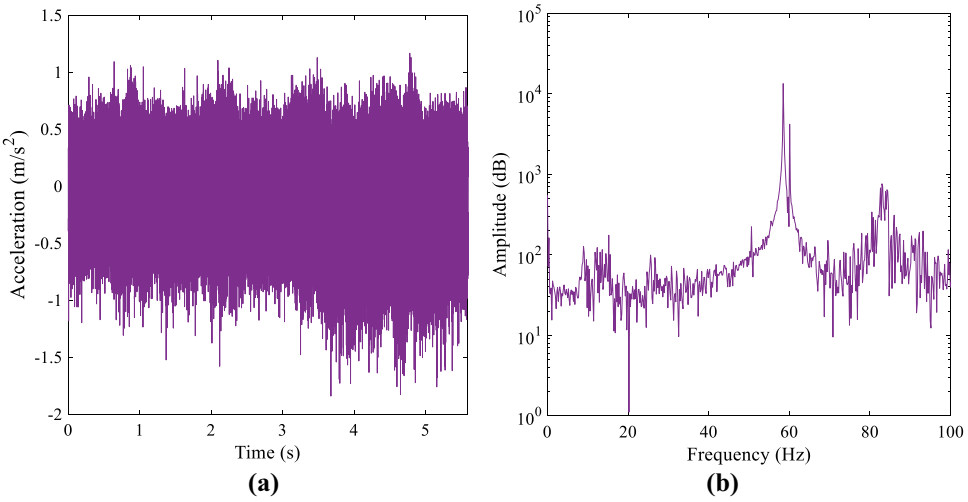

Fig. 20 Electrical unbalance fault **a** time response and **b** frequency domain

Table 6 Electrical unbalance inputs

Input	RMS	Peak	Skewness	Kurtosis	Mean	Crest factor
New motor M5	0.2975	1.1658	− 0.5685	3.8514	0.0021	3.9180

The results of the neural network were extremely satisfactory. Compared to others studies that also used ANN for similar purposes [11, 22, 26], the neural network created showed a lower error and better performance. Therefore, a high reliability neural network was created in the classification of defects of the studied electric motor.

6 Conclusions

This work presented an application of artificial neural networks aimed at classifying the operating conditions of a three-phase induction motor. The use of a neural network associated with vibration analysis was studied and verified through an experiment.

This study is also relevant to the industry. Leading companies are increasingly concerned with adapting to the "new industrial revolution," that is, industry 4.0. Predictive maintenance through vibration analysis with the aid of neural networks is a technique that fits perfectly in this context.

For the operating conditions used, the vibration signal was sensitive enough to differentiate between different conditions. However, not all defects can be satisfactorily differentiated through the vibration signal, which makes it important to add other methods such as chain or lubricant oil analysis to assist in detecting as many faults as possible.

Finally, it is highlight good results obtained with the artificial neural network for classifying operating conditions of an induction motor. All the methodology used proved to be efficient and can be used in future studies.

As a suggestion, there is an increased use of the neural network to analyze not only the vibration signal, but also other types of signals such as electric current and voltage to extend the range of operating conditions that can be detected.

Another proposal is the creation of a software based on the presented methodology that can perform measurements remotely and online. Since many devices have complicated access or need constant monitoring. Finally, more efficient transforms than FFT can be used to extract more information from the vibration signal. Recent studies are succeeding to use the transformed wavelet and Hilbert-Huang transform to analyze the vibration signal.

Acknowledgements The authors would like to acknowledge the financial support from the Brazilian agency CNPq (Conselho Nacional de Desenvolvimento Cientifico e Tecnológico), CAPES (Coordenação de Aperfeiçoamento de Pessoal de Nível Superior) and FAPEMIG (Fundação de Amparo à Pesquisa do Estado de Minas Gerais - APQ-00385-18).

Compliance with ethical standards

Conflict of interest The authors declare that they have no conflict of interest.

Appendix: Analysis of variance of the main effects

See Table 7.

Table 7 Analysis of variance of the motor response

	Source	DF	Adj SS	Adj MS	*F* value	*P* value
RSM	Condition	3	15.0113	5.00376	1144.66	0.000
	Error	12	0.0525	0.00437		
	Total	15	15.0637			
Skewness	Condition	3	0.09703	0.03234	1.38	0.297
	Error	12	0.28159	0.02347		
	Total	15	0.37862			
Mean	Condition	3	0.000003	0.000001	0.41	0.747
	Error	12	0.000025	0.000002		
	Total	15	0.000028			
Peak	Condition	3	289.06	96.354	79.08	0.000
	Error	12	14.62	1.218		
	Total	15	303.68			
Kurtosis	Condition	3	4.525	1.5083	10.24	0.001
	Error	12	1.767	0.1472		
	Total	15	6.292			
Crest factor	Condition	3	1.562	0.5206	2.29	0.130
	Error	12	2.726	0.2272		
	Total	15	4.288			

References

1. Abelém AJG, Pacheco MAC, Vellasco MMBR (1995) Modelagem de redes neurais artificiais para previsão de séries temporais. In: Simpósio brasileiro de redes neurais, 2., 1995. Universidade Federal de São Carlos
2. Abraman A (2017) situação da Manutenção no Brasil. Associação Brasileira de Manutenção e Gestão de Ativos, Documento Nacional, Rio de Janeiro: ABRAMAN
3. Almeida FA, De Paula TI, Leite RR, Gomes GF, Gomes JHF, Paiva AP, Balestrassi PP (2018) A multivariate GR&R approach to variability evaluation of measuring instruments in resistance spot welding process. J Manuf Process 36:465–479. https://doi.org/10.1016/j.jmapro.2018.10.030
4. Almeida FA, Leite RR, Gomes GF, de Freitas Gomes JH, de Paiva AP (2020) Multivariate data quality assessment based on rotated factor scores and confidence ellipsoids. Decis Support Syst. https://doi.org/10.1016/J.DSS.2019.113173
5. Barbosa LCM, Gomes G, Junior ACA (2019) Prediction of temperature-frequency-dependent mechanical properties of composites based on thermoplastic liquid resin reinforced with carbon fibers using artificial neural networks. Int J Adv Manuf Technol 105(5–6):2543–2556
6. Beale MH, Hagan MT, Demuth HB (2010) Neural network toolbox™ user's guide. The MathWorks, Natick
7. Bomfin Júnior A (2004) Implementação de uma rede neural artificial na associação de imagens do radar meteorológico e dados de descargas elétricas. INPE, São José dos Campos
8. Eswari JS, Majdoubi J, Naik S, Gupta S, Bit A, Rahimi-Gorji M, Saleem A (2020) Prediction of stenosis behaviour in artery by neural network and multiple linear regressions. Biomech Model Mechanobiol 12:1–15
9. Ferneda E (2006) Redes neurais e sua aplicação em sistemas de recuperação de informação. Ciência da Informação 35(1):25
10. Fogliatto FS, Ribeiro JLD (2009) Confiabilidade e Manutenção Industrial. Elsevier, Rio de Janeiro
11. Gaud DK, Agrawal P, Jayaswal P (2016) Fault diagnosis of rolling element bearing based on vibration & current signatures: an optimal network parameter selection. In: 2016 International conference on electrical, electronics, and optimization techniques (ICEEOT). IEEE
12. Gomes GF, de Almeida FA, Junqueira DM, da Cunha Jr SS, Ancelotti AC Jr (2019) Optimized damage identification in CFRP plates by reduced mode shapes and GA-ANN methods. Eng Struct 181:111–123
13. Gomes GF, Mendéz YAD, Alexandrino PDSL, da Cunha Jr SS, Ancelotti AC Jr (2018) The use of intelligent computational tools for damage detection and identification with an emphasis on composites–a review. Compos Struct 196:44–54
14. Hameed SS, Vaithiyanathan M, Kesavan M (2019) fault detection in single stage helical planetary gearbox using artificial neural networks (ANN) and decision tree with histogram features (No. 2019-28-0151). SAE technical paper
15. Haykin S (1994) Neural networks. A comprehensive Foundation. Prentice Hall, New Jersey
16. Lewis HG, Brown M (2001) A generalized confusion matrix for assessing area estimates from remotely sensed data. Int J Remote Sens 22(16):3223–3235
17. Lima WC, Arantes JAS (2008) Manutenção Preditiva: Caminho para a Excelência e Vantagem Competitiva. XIII, SIMPEP, Bauru, SP, Brasil
18. Marçal RA, Santos RL (2013) Medição, análise e controle de vibração em máquinas industriais: estudo de caso em uma empresa de grande porte do setor madeireiro. Universidade Tecnológica Federal do Paraná, Trabalho de Conclusão de Curso
19. Martineli E (1999) Extração de conhecimento de redes neurais artificiais. Tese de Doutorado. Universidade de São Paulo
20. Montgomery DC (2017) Design and analysis of experiments, 9th edn. Wiley, New York
21. Moubray J (2000) Manutenção Centrada em Confiabilidade (Reliability-centred Maintenance)–Edição Brasileira. SPES, Aladon Ltda, São Paulo
22. Patel JP, Upadhyay SH (2016) Comparison between artificial neural network and support vector method for a fault diagnostic in rolling element bearings. Procedia Eng 144:390
23. Sampaio GS, de Aguiar Vallim Filho AR, da Silva LS, da Silva LA (2019) Prediction of motor failure time using an artificial neural network. Sensors (Basel, Switzerland) 19(19):10
24. Silva JGB (2018) Aplicação da Análise de componentes Principais (PCA) no diagnóstico de defeitos de rolamentos através da assinatura elétrica de motores de indução. Dissertação de Mestrado em Engenharia Elétrica. Itajubá: Universidade Federal de Itajubá
25. Yetis H, Karakose M, Aydin I, Akin E (2019) Bearing fault diagnosis in traction motor using the features extracted from filtered signals. In: 2019 International artificial intelligence and data processing symposium (IDAP), September. IEEE, pp 1–4
26. Zarei J, Tajeddini MA, Karimi HR (2014) Vibration analysis for bearing fault detection and classification using an intelligent filter. Mechatronics 24(2):151